≪연구논문≫ The Journal of Optical Society of Korea (Korean Edition) Volume 4, Number 4, December 1993

Self-Organized Dynamics of Photoinduced Phase Grating formation in Optical Fibers*

Sunghyuck An
Department of Physics, Ajou University, Suwon 441-749, Korea

(Received: October 18, 1993)

The dynamics of phase grating formation with visible light in an optical fiber is investigated. Adopting a simple two-photon local bleaching model, it is shown that the grating self-organize into an ideal grating, where the writing frequency is always in the center of the local band gap, as it evolves. The evolution at each point in the fiber is described in terms of a universal parameter that reduces the coupled partial differential equations describing the system to ordinary differential equations. These equations are used to prove that there exists a fixed point of the grating growth process that corresponds to a perfectly phase-mached grating.

I. Introduction

For over a decade now it has been known that if the light of an Argon ion-laser is launched into germanosilicate optical fibers the initially high transmission drops on the time scale of seconds or minutes to very low values.[1] Early investigations showed that somehow a grating is grown in the refractive index of the glass of the fiber, phase-matched for Bragg scattering so that the light is ultimately prevented from propagating through the fiber.[1,2] A typical experimental run[3] of the growth of such a grating is shown in Fig. 1, exhibiting the oscillations in the transmission and reflection that typically accompany the general decrease in the former and rise in the latter.

A full study of this phenomenon must address two questions: First, what is the microscopic mechanism which leads to the modification of the refractive index in the fiber? Second, how does one characterize the nonlinear dynamical process which describes the growth of the grating?[4] In this paper, we shall attempt to address only the second of these questions. To do so, we require at least an approximate, phenomenological descreption of how the dielectric constant changes the fiber, in the typical experimental geometry illustrated in Fig. 2.

Though the precise microscopic mechanism which leads to these grating remains unclear, it is generally accepted that a two-photon interaction of the 488 nm laser light with an absorptive impurity band in the glass centered about 245 nm is responsible.[5-8] We present here a description based on a *local two-photon bleaching model,*[3] first suggested by Meltz et al.[7] In this model one assumes that, through the Kramers-Kronig relations, the photosensitivity originates from a bleaching of the impurity band. The justification of such models has been discussed more thoroughly in a previous study,[3,9-11] and the reader is referred to this work for a more detailed description. In the present paper we just use the result that the *local* change in dielecric function $\varepsilon(z, t)$ is related to the *local* intensity $I(z, t)$ through a two-photon process, *viz.* $\partial\varepsilon(z, t)/\partial t \propto I^2(z, t)$, and explore its consequences.

II. Basic equations

In this section we first discuss how a given grating at time t affects the propagation of light through the fiber. We neglect effects specifically related to the fiber mode profiles, and assume that the only relevant spa-

* This work was supported by Ajou university research fund and by the Basic Science Research Institute Program of the Korea Ministry of Education (BSRI-92-237).

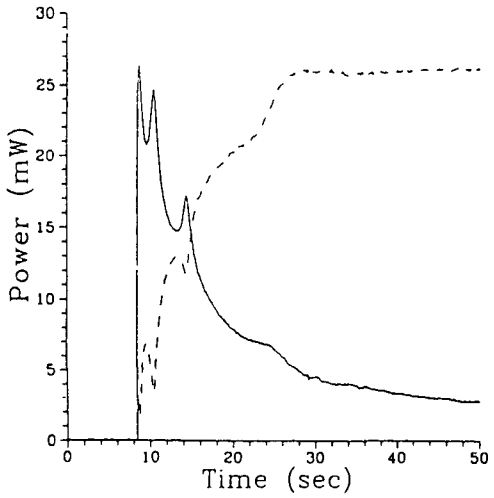

Fig. 1. Experimental results shown in Ref. 3. The solid and dashed lines show the transmitted and reflected powers, respectively, as time increases. The gradual damping of the oscillation is due to the fiber heating.

tial coordinate of the system is that of the fiber axis, z. In the pristine fiber light propagates with a wave number $k=(\omega/c)\sqrt{\bar{\varepsilon}}$, where ω is the incident light frequency and $\bar{\varepsilon}$ is the initial uniform effective dielectric constant. At a later time, the effective dielectric constant can be written as

$$\varepsilon(z,\ t)=\bar{\varepsilon}+\Delta\varepsilon(z,\ t), \tag{1}$$

where $\Delta\varepsilon(z,\ t)$ is the photo-induced modification. Retaining grating terms of spatial frequencies $\pm 2k$, which may give Bragg matched reflection, we can write $\Delta\varepsilon$ generally as

$$\begin{aligned}\Delta\varepsilon(z,\ t)&=\varepsilon_0(z,\ t)+\varepsilon_2(z,\ t)e^{2ikz}+\varepsilon_2^*(z,\ t)e^{-2ikz}\\&=\varepsilon_0(z,\ t)+2|\varepsilon_2(z,\ t)|\cos(2kz+\phi(z,\ t)),\end{aligned} \tag{2}$$

where $\varepsilon_0(z,\ t)$ is the modification to the background index and $|\varepsilon_2(z,\ t)|$ and $\phi(z,\ t)$ are the amplitude and phase of a grating, respectively. We assume that no linear absorption is induced and thus that $\Delta\varepsilon(z,\ t)$, $\varepsilon_0(z,\ t)$, and $\phi(z,\ t)$ are real.

We write the electric field inside the fiber as

$$E(z,\ t)=e(z,\ t)e^{-i\omega t}+c.c., \tag{3}$$

with

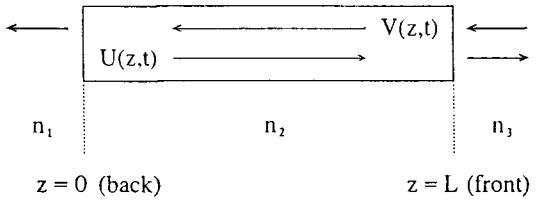

Fig. 2. Schematic of the geometry we consider. The indices of refraction are given by n_1 for $z<0$, n_2 for $0<z<L$, and n_3 for $z>L$. Note that the light enters from the right-hand side.

$$e(z,\ t)=U(z,\ t)e^{ikz}+V(z,\ t)e^{-ikz}, \tag{4}$$

where $U(z,\ t)$ and $V(z,\ t)$ are the complex amplitudes of the right and left traveling waves respectively (see Fig. 2). Since the photoinduced gratings change on time scales typically much longer than the fiber round trip time L/c, where L is the length of the fiber, at any time t we can take $e(z,\ t)$ to be a solution of the wave equation describing stationary fields,

$$\left[\frac{\partial^2}{\partial z^2}-\frac{\omega^2}{c^2}\varepsilon(z,\ t)\right]e(z,\ t)=0. \tag{5}$$

Initially, before any photoinduced change in $\varepsilon(z,\ t)$, U and V are of course uniform. For the weak gratings that are typically induced, we assume that the scattering of light from the right to the left, and vice versa, can be described by fields $U(z,\ t)$ and $V(z,\ t)$ that are slowly varying in space on the time scale of the wavelength $2\pi/k$. Using Eq.(4) in Eq.(5) and adopting the slowly varying envelope approximation, we find the *coupled mode equations*

$$\begin{aligned}\frac{\partial U(z,\ t)}{\partial z}&=\frac{ik}{2\bar{\varepsilon}}\left[\varepsilon_0(z,\ t)U(z,\ t)+\varepsilon_2(z,\ t)V(z,\ t)\right]\\\frac{\partial V(z,\ t)}{\partial z}&=-\frac{ik}{2\bar{\varepsilon}}\left[\varepsilon_0(z,\ t)V(z,\ t)+\varepsilon_2^*(z,\ t)U(z,\ t)\right].\end{aligned} \tag{6}$$

To solve Eqs.(6) and determine the electric field throughout the fiber at any given time t, we must specify the physically appropriate boundary conditions. If we choose the geometry of the system as shown in Fig. 2, where for convenience the light is taken to be coming from the right, then the boundary conditions at the back ($z=0$) and front ($z=L$) ends of the fiber are given by

$$U(0,\ t)=r_{21}V(0,\ t), \tag{7}$$

and

$$e_{in}=\frac{1}{t_{32}}\left[V(L,\ t)e^{-ikL}-r_{23}U(L,\ t)e^{ikL}\right], \tag{8}$$

where e_{in} is the input field at $z=L^{+}$, which is assumed to be constant for $t>0$, and r_{ij} and t_{ij} are the effective reflection and transmission coefficients at the corresponding interfaces. If a plane wave model is used to describe the reflection and transmission at the interfaces, then the r_{ij} and t_{ij} are given by the well-known Fresnel coefficients

$$r_{ij}=\frac{n_i-n_j}{n_i+n_j}$$
$$t_{ij}=\frac{2n_i}{n_i+n_j}, \tag{9}$$

where the effective indices of refraction are given by n_1 for $z<0$, $n_2(=\sqrt{\bar{\varepsilon}})$ for $0<z<L$, and n_3 for $z>L$. Note that we have assumed $\Delta\varepsilon\ll\bar{\varepsilon}$, so effective index of only the unexposed fiber appears in Eqs.(9).

Eqs.(6-9) describe how a given grating influences the fields at any instant in time. Next we discuss how the field modify the grating at each position of the fiber. Although the microscopic origin of the grating formation is not yet clear, experimental evidence indicates that at least the initial grating growth can be described by a time rate of change of $\Delta\varepsilon$ proportional to the square of the intensity.[6] A model in which, say, two-photon absorption leads to a change in the properties of defect sites with linear absorption bands in the ultraviolet,[5,7] perhaps shifting those bands, would through the Kramers-Kronig relation lead to a change in the (essentially real) dielectric constant at optical frequencies consistent with the observed initial grating rate of change. In its simplest form, this model yields a dynamical equation for the photoinduced change $\Delta\varepsilon(z,\ t)$ of the form[3]

$$\frac{\partial}{\partial t}\Delta\varepsilon(z,\ t)=AI^2(z,\ t), \tag{10}$$

where A is a real constant and saturation effects associated with depletion of the original defect sites are neglected; the local intensity is proportional to

$$I(z,\ t)=|e(z,\ t)|^2. \tag{11}$$

For most of this paper we will adopt Eq.(10), sometimes called the *local two-photon bleaching model*, and explore its consequences. We mention that, even if Eq. (10) is accepted as the model for the permanent change in the dielecric constant, transient phenomena such as fiber heating can quantitatively affect the dynamics of gratng growth.[3] Such effects, which do not seem to modify the essential qualitative dynamics of grating formation, we neglect here.

Substituting Eqs.(2) and (4) into Eq.(10) and neglecting the non-phase matched terms involving e^{4ikz} and e^{-4ikz}, we have

$$\frac{\partial\varepsilon_0(z,\ t)}{\partial t}=A[(|U(z,\ t)|^2+|V(z,\ t)|^2)$$
$$+2|U(z,\ t)^2|V(z,\ t)|^2]$$
$$\frac{\partial\varepsilon_2(z,\ t)}{\partial t}=2A(|U(z,\ t)|^2+|V(z,\ t)|^2)U(z,\ t)V^{*}(z,\ t), \tag{12}$$

which are subject to the initial conditions

$$\varepsilon_0(z,\ 0)=\varepsilon_2(z,\ 0)=0. \tag{13}$$

Equations (12) and the initial conditions (13), combined with Eqs.(6) and the boundary conditions given by Eqs. (7) and (8), define the nonlinear dynamics of the system. We note the $U(z,\ t)$ and $V(z,\ t)$ change $\varepsilon_0(z,\ t)$ and $\varepsilon_2(z,\ t)$ locally, but that modifications of the dielectric constant change $U(z,\ t)$ and $V(z,\ t)$ globally. As a result, the dynamics of the electric field and grating are so intricately connected that it is difficult to separate one from the other. In the section 5, however, we show that in homogeneous models of the form of Eq.(10) there exists a *universal evolution parameter* which makes it possible to essentially decouple the local and non-local aspects of the dynamics of the system. Using this parameter we are able to transform the coupled partial differential equations into coupled *ordinary* differential equations, which of course vastly simplify the problem.

III. Numerical Calculations

We use a fourth-order Runge-Kutta method to solve numerically the coupled partial differential equations defined in Sec. 2. In Fig. 3 we plot the transmission of the light through the fiber as a function of time.

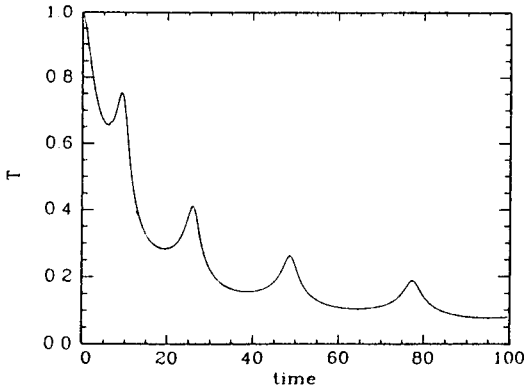

Fig. 3. Transmissivity as a function of time (arbitrary units) in a numerical simulation for a fiber of 30 cm length, and $(n_1, n_2, n_3)=(1, 1.5, 1)$.

It shows that the transmission is decreasing in time with the oscillations, showing good agreement with the experimental observations (see, Fig. 1).

In Fig. 4(a) we plot the transmission versus time when we assume no Fresnel reflection at the front end of the fiber initially (i.e., we set $r_{23}=0$ at $t=0$). The boundary condition at the front end of the fiber (i.e., Eq. 8) does not contribute to the transmission in this case, and as a result we see that the osillatory behavior shown in Fig. 3 does not appear and the transmission drops monotonically. On the other hand, in Fig. 4(b) we plot the transmission versus time when we use the same boundary conditions as in the case of Fig. 3 initially, but at $t=20$ we set $r_{21}=0$ (i.e., the Fresnel reflection at the far end of the fiber is removed at this time). We see that the grating appears to stop growing and the transmission shows only the oxcillatory behavior in time. Therefore we qualitatively conclude that the overall decrease of the transmission in Fig. 3 is due to the Fresnel reflection at the far end, and the oscillations are due to the interference between the light reflected directly from the front end surface and that reflected from the grating which is only moving.

In Figs. 5(a)-(c) we plot ε_0, $|\varepsilon_2|$, and the phase of ε_2, as a function of position z at $t=100$. They all show monotonically increasing functions of z. From Fig. 5(c) we see that grating is highly chirped, and the grating phase ϕ is fixed at far end of the fiber $z=0$, which comes from the initial condition (13).

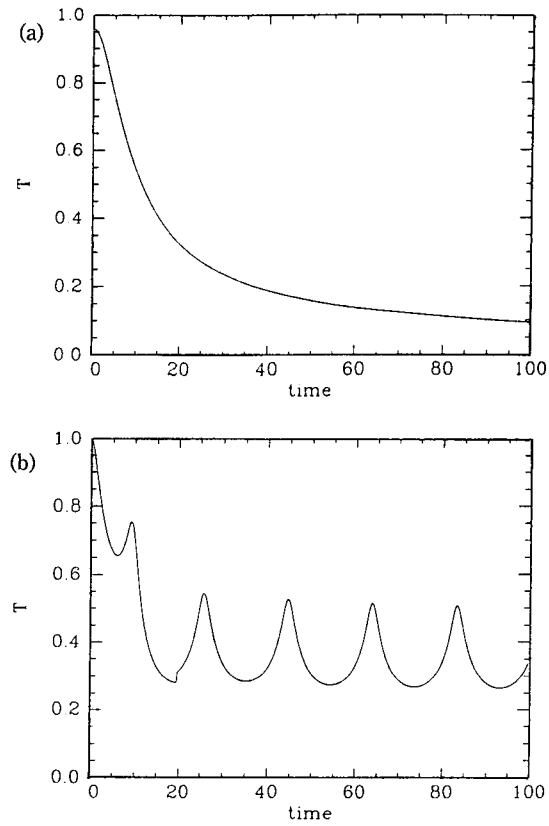

Fig. 4. (a) Transmissivity as a function of time when $r_{23}=0$ at $t=0$. (b) Transmissivity as a function of time when $r_{21}=0$ at $t=20$.

In Fig. 6 we plot the frequency response of the grating which was written by the light of frequency ω_0. We stop growing the grating at $t=100$ and put a probe beam of frequency ω into the front surface of the fiber to study the reflectivity as a function of frequency. We see that the band width of the spectrum is order of 100 MHz. The narrow response of the grating also implies that it is almost perfectly phase matched to the writing radiation. In Fig. 7 we plot the frequency response of a uniform grating, when its maximum refectivity is equal to that of Fig. 6, and comparing it with Fig. 6 we indeed notice that the grating of Fig. 6 is perfectly phase matched.

IV. The gap parameter

Before we try to solve the coupled mode equations

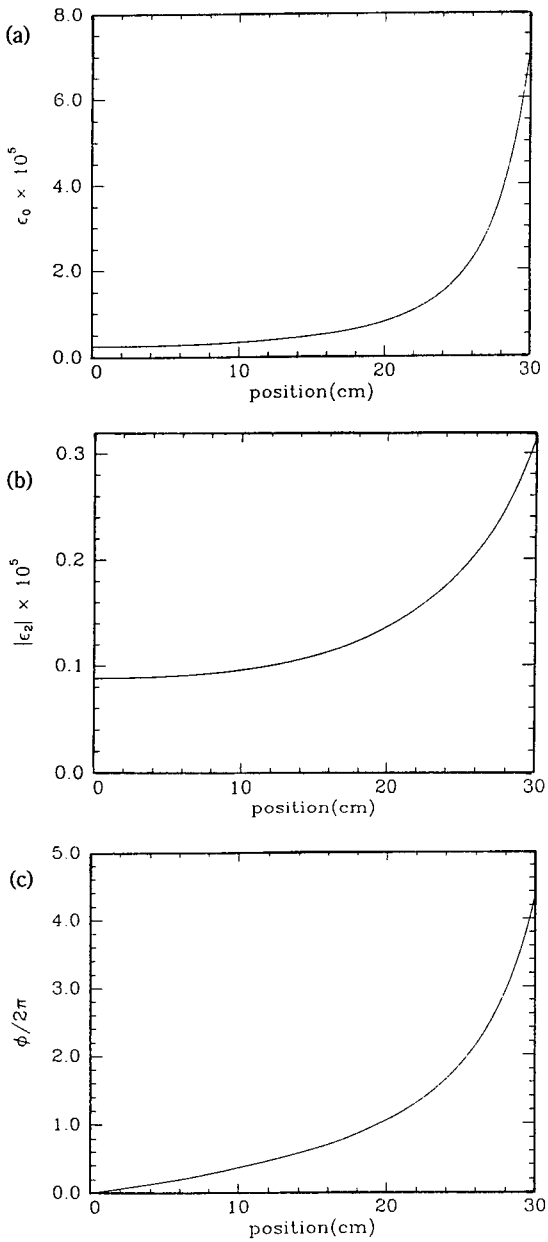

Fig. 5. Plots of (a) ε_0, (b) $|\varepsilon_2|$, and (c) ϕ as a fuction of position z at $t=100$.

analytically, it turns out to be useful to rewrite these equations in a more concise formalism. To do this, we first write the coupled mode equations (6) as

$$\frac{\partial U(z,\ t)}{\partial z}=i\sigma(z,\ t)U(z,\ t)+i\kappa(z,\ t)e^{i\phi(z,\ t)}V(z,\ t)$$

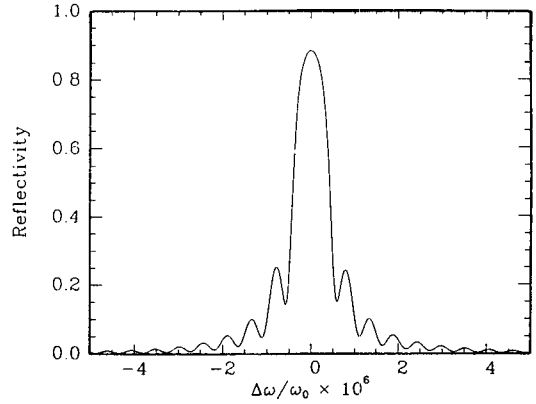

Fig. 6. Reflectivity as a function of wavelength for the grating of Fig.4 at $t=100$.

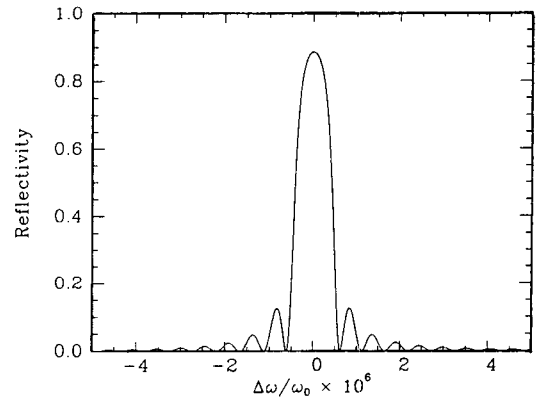

Fig. 7. Reflectivity as a function of wavelength for a uniform grating when its maximum reflectivity is equal to that of Fig. 7.

$$\frac{\partial V(z,\ t)}{\partial z}=-i\sigma(z,\ t)V(z,\ t)-i\kappa(z,\ t)e^{-i\phi(z,\ t)}U(z,\ t),\quad(14)$$

where the grating fields $\sigma(z,\ t)$ and $\kappa(z,\ t)$ are defined by

$$\sigma(z,\ t)=\frac{k}{2\bar{\varepsilon}}\,\varepsilon_0(z,\ t)$$

$$\kappa(z,\ t)=\frac{k}{2\bar{\varepsilon}}\,|\varepsilon_2(z,\ t)|.\quad(15)$$

We next transform $U(z,\ t)$ and $V(z,\ t)$ to the field amplitudes $u(z,\ t)$ and $v(z,\ t)$ in the *grating frame* such that

$$U(z,\ t)=u(z,\ t)e^{i\phi(z,\ t)/2}$$

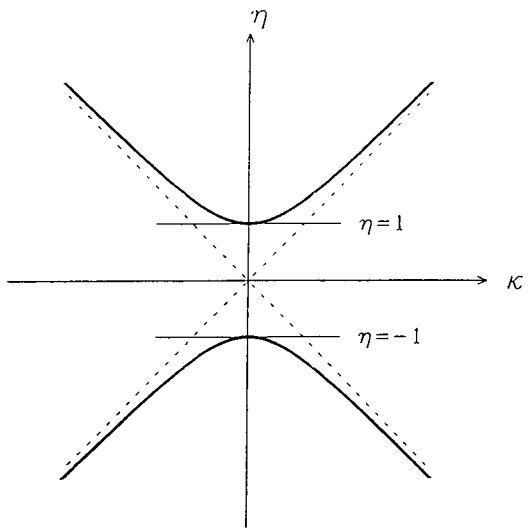

Fig. 8. Plot of η versus k given by Eq.(20)

$$V(z,\ t)=v(z,\ t)e^{-i\phi(z,\ t)/2}. \tag{16}$$

Then substituting Eqs.(16) into Eqs.(14), defining the *effective length* y at each time

$$y=\int_0^z \kappa(z',\ t)dz', \tag{17}$$

and introducing the *gap parameter* η,

$$\eta=\frac{1}{\kappa(z,\ t)}\left[\sigma(z,\ t)-\frac{1}{2}\frac{\partial\phi(z,\ t)}{\partial z}\right] \tag{18}$$

we can finally rewrite the coupled mode equations as

$$\begin{aligned}\frac{\partial u}{\partial y}&=i\eta u+iv\\ \frac{\partial v}{\partial y}&=-i\eta v-iu.\end{aligned} \tag{19}$$

We notice that the variable z does not appear in Eqs. (19), and intead y plays the role of an effective spatial coordinate. Moreover all the grating fields (i.e., σ, κ, and ϕ) are combined in a new field η, and we thus only need to analyze the effect of any grating field on η to understand its role in the coupled mode equations.

To see the qualitative behavior of the fields u and v as a function of η, we consider the special case of uniform η. Then we easily find that u and v are given by the linear combinations of e^{iky} and e^{-iky}, where k is given by

$$k=\pm\sqrt{\eta^2-1}\ . \tag{20}$$

From Eq.(20) we see that if $|\eta|>1$, the fields are described by sinusoidal functions, and thus forward and backward waves propagate with amplitudes determined by the boundary conditions. In fact, as $|\eta|\to\infty$, the coupled mode equations become totally decoupled, and u and v propagate independently (see Fig. 8). On the other hand if $|\eta|<1$ (defining the *stop gap*), u and v are described by hyperbolic functions which are non propagating (the edges of stop gap are defined by $\eta=\pm 1$). Moreover, in the middle of the stop gap (i.e., $|\eta|\to 0$) we exactly satisfy the Bragg condition. Therefore in order to get the strongly Bragg-matched reflected light we expect that η must be in the region of the stop gap.

V. Reduction of the dynamics

The solution of the set of coupled partial differential equations (6, 12) is facilitated by the introduction of new variables to define the state of the electromagnetic field. We put

$$\begin{aligned}s_1&=2Re[v^*(z,\ t)u(z,\ t)]\\ s_2&=2Im[v^*(z,\ t)u(z,\ t)]\\ s_3&=|v(z,\ t)|^2-|u(z,\ t)|^2\\ s_0&=|v(z,\ t)|^2+|u(z,\ t)|^2.\end{aligned} \tag{21}$$

Note that these are not all independent, but they satisfy the relation

$$s_0^2=s_1^2+s_2^2+s_3^2. \tag{22}$$

If s_1, s_2 and s_3 are specified at a given $(z,\ t)$, then $u(z,\ t)$ and $v(z,\ t)$ may be determined except for an overall phase factor. We begin by writing the coupled mode equations (6) in terms of s-variables:

$$\begin{aligned}\frac{\partial s_0}{\partial y}&=2s_2\\ \frac{\partial s_1}{\partial y}&=-2\eta s_2\\ \frac{\partial s_2}{\partial y}&=2\eta s_1+2s_0\\ \frac{\partial s_3}{\partial y}&=0.\end{aligned} \tag{23}$$

The two-photon equations (12) can be rewritten as

$$\frac{\partial \sigma}{\partial t} = s_0^2 + \frac{1}{2}(s_1^2 + s_2^2)$$
$$\frac{\partial \kappa}{\partial t} = s_0 s_1$$
$$\kappa \frac{\partial \phi}{\partial t} = s_0 s_2, \tag{24}$$

where the coefficient A in Eqs.(12) is absorbed in time variable t. The initial conditions (13) become

$$\sigma(z,\ 0) = \kappa(z,\ 0) = \phi(z,\ 0) = 0, \tag{25}$$

where the initial condition on ϕ is chosen for later convenience. To complete the rewriting of our dynamical equations (6-8, 12-13) in terms of these new variables, we must consider the boundary conditions (7-8). Equation (7) is easily written as a condition on ratios of the s-parameters,

$$s_1(0,\ t)/s_3(0,\ t) = 2r_{21}/(1-r_{21}^2)$$
$$s_2(0,\ t)/s_3(0,\ t) = 0$$
$$s_0(0,\ t)/s_3(0,\ t) = (1+r_{21}^2)/(1-r_{21}^2), \tag{26}$$

where the third follows from the first two and Eq.(22). The boundary condition (8) may also be written in terms of our new variables, but it is more complicated; we defer its expression to later in this section.

The last of Eqs.(23) expresses the fact that the energy flux through the fiber is independent of position; from it we may write

$$s_3 = s_3(t). \tag{27}$$

This holds because we neglect any effect of absorption on the light propagation. Such absorption, though ultimately responsible for the change in the dielectric constant that leads to grating formation, is very weak, and its neglect on light propagation, implicit in the form of our coupled mode equations (6) and the parameters in those equations, is well justified.

Since s_3 does not depend on the variable z, we are led to simplify our equations by dividing both sides of Eqs.(23) by s_3 to obtain

$$\frac{\partial \bar{s}_0}{\partial y} = 2\bar{s}_2$$
$$\frac{\partial \bar{s}_1}{\partial y} = -2\eta \bar{s}_2$$
$$\frac{\partial \bar{s}_2}{\partial y} = 2\eta \bar{s}_1 + 2\bar{s}_0, \tag{28}$$

where the $\bar{s}$-bariables are defined as

$$\bar{s}_o = \frac{s_0}{s_3},\ \bar{s}_1 = \frac{s_1}{s_3},\ \bar{s}_2 = \frac{s_2}{s_3}. \tag{29}$$

We can also write Eqs.(24) in terms of the $\bar{s}$-variables

$$\frac{\partial \sigma}{\partial \tau} = \bar{s}_0^2 + \frac{1}{2}(\bar{s}_1^2 + \bar{s}_2^2)$$
$$\frac{\partial \kappa}{\partial \tau} = \bar{s}_0 \bar{s}_1$$
$$\kappa \frac{\partial \phi}{\partial \tau} = \bar{s}_0 \bar{s}_2, \tag{30}$$

where a new time variable τ is defined as

$$\tau = \int_0^t s_3^2(t')dt'. \tag{31}$$

We now seek a solution of our equations involving an evolution of the grating fields of the form

$$\sigma = \tau \bar{\sigma}(\tau z)$$
$$\kappa = \tau \bar{\kappa}(\tau z)$$
$$\phi = \bar{\phi}(\tau z), \tag{32}$$

which satisfies the initial conditions (25) as long as $\bar{\phi}(0) = 0$. For this assumed form for the grating fields, y and η in Eqs.(17) and (18) can be written respectively as

$$y = \int_0^x \bar{\kappa}(x')dx' = y(x)$$
$$\eta = \frac{\bar{\sigma}(x) - \frac{1}{2}\frac{d\bar{\phi}(x)}{dx}}{\bar{\kappa}(x)} = \eta(x), \tag{33}$$

where the *universal evolution parameter* x is defined by

$$x = \tau z. \tag{34}$$

That is, if the grating fields do evolve according to the form Eq.(32), then the evolution of y and η at any point in the fiber is similar to the evolution of those quantities at every other point in the fiber. In particular, the grating parameter η goes through the same evolution history at each point in the fiber, points at the input end of the fiber (large z) simply running through this history at a faster rate than points near

the far end of the fiber (small z).

Since y and η depend explicitely only on x for the proposed solution (32), from Eqs. (28) we are led to seek $\bar{s}$-variable evolution which also depend only on x, i.e.,

$$\bar{s}_0=\bar{s}_0(x),\quad \bar{s}_1=\bar{s}_1(x),\quad \bar{s}_2=\bar{s}_2(x). \tag{35}$$

Then, using the assumed forms (32, 35), we find

$$\frac{d\bar{s}_0(x)}{dx}=2\bar{\kappa}(x)\bar{s}_2(x)$$

$$\frac{d\bar{s}_1(x)}{dx}=-2\bar{\kappa}(x)\eta(x)\bar{s}_2(x)$$

$$\frac{d\bar{s}_2(x)}{dx}=-2\bar{\kappa}(x)\eta(x)\bar{s}_2(x)+2\bar{\kappa}(x)\bar{s}_0(x) \tag{36}$$

are required to satisfy Eqs.(28), and

$$\bar{\sigma}(x)=\frac{1}{x}\int_0^x\left[\bar{s}_0^2(x')+\frac{1}{2}(\bar{s}_1^2(x')+\bar{s}_2^2(x'))\right]dx'$$

$$\bar{k}(x)=\frac{1}{x}\int_0^x\bar{s}_0(x')\bar{s}_1(x')dx' \tag{37}$$

and

$$\frac{d\bar{\phi}(x)}{dx}=\frac{1}{x}\frac{\bar{s}_0(x)\bar{s}_2(x)}{\bar{\kappa}(x)} \tag{38}$$

are required to satisfy Eqs.(30). The boundary condition (26) becomes an initial condition to which Eqs.(36-38) are subject,

$$\bar{s}_1(0)=\frac{2r_{21}}{1-r_{21}^2},\quad \bar{s}_2(0)=0. \tag{39}$$

So we see that gratings of the form (32), and electric fields of the form specified implicitly by (35), do indeed describe a solution of the coupled partial differential equations (6, 12), which are subject to the boundary conditions (7), as long as Eqs.(36-37) are satisfied, subject to the initial condition (39) and the relations (33, 38). The problem of solving the coupled partial differential equations has been replaced by the problem of solving the two ordinary, integro-differential equations (36-37). It is clear from this reduction that the gap parameter η and $\bar{s}$-variables at each point in the fiber, except $z=0$, evolve in exactly the same way when measured by the universal parameter x. With respect to actual time, of course, the points at the front end of the fiber evolve more quickly, as expected since it is that region from which light is last excluded as the grating grows. What was unexpected and we believe is surprising is that, once this effect is included by characterizing the evolution in terms of the parameter x, the grating fields and electric field evolve in such a similar manner (Eqs. 32, 35) at each point in the fiber.

The barred functions can be determined numerically, and are independent of both the length of the fiber and the index n_3, since the boundary condition (7) has been used only. To determine $s_3(t)$ and thus complete the determination of the grating and field, we must use the other boundary condition (8). From Eqs. (21, 29) we have

$$|U(L,\ t)|^2=\frac{1}{2}s_3(t)[\bar{s}_0(\tau L)-1]$$

$$|V(L,\ t)|^2=\frac{1}{2}s_3(t)[\bar{s}_0(\tau L)+1] \tag{40}$$

and substituting Eqs.(40) into Eq.(8) we find

$$\begin{aligned}\frac{t_{32}^2|e_{in}|^2}{s_3(t)}&=\frac{1}{2}(1+r_{23}^2)\bar{s}_0(\tau L)+\frac{1}{2}(1-r_{23}^2)\\&\quad+r_{23}[\bar{s}_2(\tau L)\sin(2kL+\bar{\phi}(\tau L))\\&\quad-\bar{s}_1(\tau L)\cos(2kL+\bar{\phi}(\tau L))]\\&\equiv F(\tau,\ L).\end{aligned} \tag{41}$$

Finally substituting Eq.(41) into Eq.(31) we have

$$\int_0^\tau F^2(\tau',\ L)d\tau'=t_{32}^2|e_{in}|^4t. \tag{42}$$

After the barred functions have been numerically determined, Eq.(42) may be used to find τ in terms of t, from which (see Eq. 31) $s_3(t)$ may be determined for the particular length of fiber and n_3 under consideration. Inverting Eq.(42) numerically to find $\tau(t)$, the complete solutions for the grating and field are determined. With this in hand, all physical quantities of interest can be calculated. For example, the transmission of the fiber is give by

$$\begin{aligned}T(t)&=\frac{n_1}{n_3}\left|\frac{e_{out}(t)}{e_{in}}\right|^2\\&=\frac{n_1}{2n_3}\frac{t_{21}^2t_{32}^2}{F(\tau,\ L)}(1+\bar{s}_0(0)),\end{aligned} \tag{43}$$

where $e_{out}(t)=t_{21}V(0,\ t)$ is the transmitted field at $z=$

0^-, and in deriving the second line of Eq.(43) we have used Eqs.(40-41).

VI. Fixed point

To see qualitatively how the state of the grating in the fiber evolves, we study the evolution of the parameters η and μ, where

$$\mu=\frac{1}{2\kappa^2(z,\ t)}\frac{\partial\kappa(z,\ t)}{\partial z}$$
$$=\frac{1}{2\bar{\kappa}^2(x)}\frac{d\bar{\kappa}(x)}{dx}\equiv\mu(x), \tag{44}$$

the second equality following from the forms (32). From Eqs.(37) and (39), we find

$$\eta(0)=\frac{r_{21}}{2(1+r_{21}^2)},\quad \mu(0)=0. \tag{45}$$

In Fig. 9 we show a plot of μ versus η, with x as a parameter, determined from a numerical solution of Eqs.(36-37) with $n_1=1$ and $n_2=1.5$. From Fig. 9 we see, since $x\to\infty$ as $t\to\infty$ for all points of the fiber except $z=0$, that all points of the fiber except the very far end tend asymtotically to the state $\eta=0$, $\mu=1/2$. This then identifies a fixed point, or attractor, for the state of growth of the grating. Numerical investigations indicate that there exists only one fixed point which is independent of r_{21}; indeed, this independence and the stability of the fixed point may be examined analytically. To do this we find, using Eqs.(36-37) and the definitions (33) and (44),

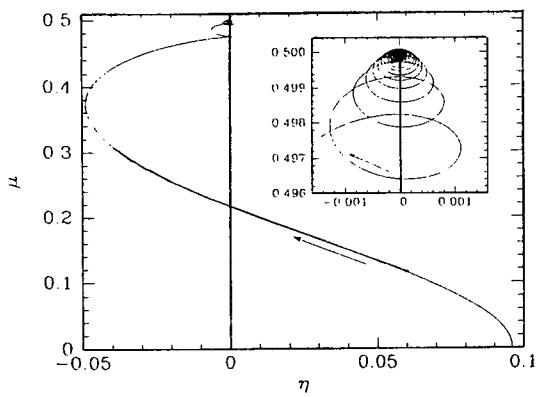

Fig. 9. Plot of μ versus η as x varies from 0 to ∞ for $n_1=1$ and $n_2=1.5$. Note that $(\eta,\ \mu)\to(0,\ 1/2)$ as $x\to\infty$. The arrows in the figure denote the directionof increasing x.

$$\frac{d\eta}{d\bar{\phi}}=\frac{\bar{s}_1^2-\bar{s}_2^2}{2\bar{s}_0\bar{s}_2}+\mu-\frac{2\bar{s}_1}{\bar{s}_2}\eta$$
$$\frac{d\mu}{d\bar{\phi}}=\frac{\bar{s}_1}{\bar{s}_0}-\eta-\frac{2\bar{s}_1}{\bar{s}_2}\mu. \tag{46}$$

From Eq.(45) we see that $0\le\eta(0)<0.25$, so we consider the general behavior of η, μ in the neighborhood of $\eta=0$ by using the solutions of Eqs.(36) at $\eta=0$. Those solutions, which satisfy the initial condition (39), are

$$\bar{s}_1\approx\left(\frac{2r_{21}}{1-r_{21}^2}\right)$$
$$\bar{s}_2\approx\left(\frac{1+r_{21}^2}{1-r_{21}^2}\right)\sinh\left[2\int_0^x\bar{\kappa}(x')dx'\right]. \tag{47}$$

Using Eqs.(47) in Eqs.(46), we find

$$\frac{d\eta}{d\bar{\phi}}=\tilde{\mu}-\frac{2\bar{s}_1}{\bar{s}_2}\eta$$
$$\frac{d\tilde{\mu}}{d\bar{\phi}}=-\eta-\frac{2\bar{s}_1}{\bar{s}_2}\tilde{\mu}, \tag{48}$$

in the limit $x\to\infty$, where $\tilde{\mu}=\mu-1/2$. That is, $(\eta,\ \tilde{\mu})$ behave like the conjugate variables of a damped harmonic oscillator, reaching a stable steady state $(\eta,\ \tilde{\mu})=(0,\ 0)$ as $x\to\infty$. The universality implies that at each point in the fiber the grating state, specified by η and μ goes through the same history, but at a different rate. Thus we see that the dynamical process approaches a fixed point corresponding to a perfectly phase-matched grating, with the region of the fiber near the input moving faster towards that attractor than the regions further away.

VII. Conclusions

In summary, there is interesting grating dynamics to be investigated in the "internal writing" geometry shown in Fig. 2. If a local two-photon bleaching model is adopted, the gratings self-organize into effectively "ideal" gratings, in the sense that they adjust themselves so that the center of the local band gap is at the writing frequency. This corresponds to a fixed point of the state of grating growth. More generally, for all homogeneous growth equation of the form (10) a uni-

versal parameter describes the evolution of the grating at every point, with each point in the grating developing in essentially the same way. Extensions of the kind of approach we have developed here to other geometries and material dynamics are underway.[11]

References

[1] K. O. Hill, Y. Fujii, D. C. Johnson and B. S. Kawaski, Appl. Phys. Lett. **32**, 647 (1978).

[2] B. S. Kawasaki, K. O. Hill, D. C. Johnson and Y. Fujii, Opt. Lett. **3**, 66 (1978).

[3] V. Mizrahi, S. LaRochelle, G. I. Stegeman and J. E. Sipe, Phys. Rev. A **43**, 433 (1991).

[4] J. Bures, J. Lapierre and D. Pascale, Appl. Phys. Lett. **37**, 660 (1980).

[5] M. J. Yuen, Appl. Opt. **21**, 136 (1982).

[6] D. K. W. Lam and B. K. Garside, Appl. Opt. **20**, 440 (1981).

[7] G. Meltz, W. W. Morey and W. H. Glenn, Opt. Lett. **14**, 823 (1989).

[8] D. P. Hand and P. St. Russell, Opt. Lett. **15**, 102 (1990).

[9] C. M. de Sterke, S. An, and J. E. Sipe, Opt. Comm. **83**, 315 (1991).

[10] S. An and J. E. Sipe, Opt. Lett. **16**, 1478 (1991).

[11] S. An and J. E. Sipe, Opt. Lett. **17**, 490 (1992).

광 섬유내의 광유도 위상격자가 형성되는 자기조직 역학에 관한 연구

안 성 혁

아주대학교 물리학과

(1993년 10월 18일 받음)

본 논문에서는 광섬유에 아르곤 레이저 빔이 입사될 때 생기는 위상격자 형성에 관한 역학을 다룬다. 간단한 쌍광자 표백모델(two-photon bleaching model)을 이용하여 위상격자가 시간이 지남에 따라 이상적인(ideal) 격자로 자기조직됨(self-organized)을 보인다. 광섬유의 각점에서의 시간에 따른 상태전개는 하나의 보편 매개변수(universial parameter)에 의해 나타내어지고 또한 이 광섬유계를 기술하는 연립 편미분 방정식이 이 매개변수에 의해 연립 상 미분 방정식으로 간소화 된다. 이 연립 상 미분 방정식을 이용하여 위상격자가 자라나는 상태는 한 고정점(a fixed point)를 향해 가는 과정이고 이 고정점은 완벽히 위상맞춤(phase-matched)된 격자에 해당된다는 것을 보인다.